УДК 621.373.12; 621.396.962.2

Signals Features from Distributed Targets of Autodyne SRR with Simultaneous Pulse Amplitude and Linear Frequency Modulations

Noskov V. Ya.[1], *Ignatkov K. A.*[1], *Chupahin A. P.*[1], *Vasiliev A. S.*[2], *Fateev A. V.*[2], *Smolskiy S. M.*[3]

[1]Ural Federal University, Ekaterinburg, Russia
[2]O.Ya. Usikov Institute for Radiophysics and Electronics, Kharkiv, Ukraine
[3]National Research University "Moscow Power Engineering Institute", Moskow, Russia

E-mail: *noskov@oko-ek.ru*

A mathematical model for signals description of the autodyne short-range radar (ASRR) with the simultaneous pulse amplitude modulation (PAM) and the linear frequency modulation (FM) is considered. The peculiarities of signal formation are described, which are obtained from the radar distributed object in the form of an ensemble of an arbitrary number of point-type reflectors. Signal calculations are carried out by the offered approach of the step method for the case of two point reflectors on the radar object located at various distances from ASRR. The distinctive signal properties formed at reception of the first and further emissions reflected form the radar object are established. After sending of the probe emission, the reception of the first reflected emission from the set of shining points is accompanied by linear signal superposition formation from separate reflectors. The reception of further reflections causes an appearance of combinational signal interaction from separate reflectors. The character and degree of such an interaction is defined by the feedback parameter of ASRR, which depends on the autodyne frequency deviation and delay time of reflected emission. Results of ASRR experimental investigations with simultaneous PAM and the linear FM are obtained using the oscillating module made on the Gunn diode of 8mm-range.

Key words: autodyne; autodyne effect; autodyne signal; radio pulse autodyne; autodyne with frequency modulation; feedback parameter; short-range radar.

Introduction

When using in autodyne short range radar (ASRR) of the simultaneous pulse amplitude modulation (PAM) and frequency modulation (FM), we provide the essential ASRR noise-immunity and a possibility to form the near and far detection zones' boundaries in the range [1]. Besides, autodyne (AD) operation intermittence increases the ASRR operation secrecy as well as essentially decreases the power consumption. Owing to mentioned advantages, the radio pulse ADs are widely used in the military devices, in various sensors of collision avoidance with obstacles in the motor-car and railway transport, in radio wave sensors of guarding destination and in many other applications [2–5].

In the real ASRR operation conditions, the autodyne interacts with the emission reflected from the distributed, spatially-non-uniform radar target. Nevertheless, all published investigations known to us and devoted to studying of AD signal features from the distributed target, were mainly performed in connection with continuous wave AD without PAM [6]. A series of such research results is obtained separately for the radio pulse AD and the FM autodyne. At that, signal properties are studied at simultaneous utilization of PAM and FM on an example of the only elementary point reflector only (see our paper [1,7,8]). In this connection, it is expedient to examine the case when the emission reflected from the distributed target affects on the ASRR with PAM and FM. Results of these investigations necessary for AD correct application in SRR and for widening of its functional opportunities are described in this paper.

1 Main Equations for an Analysis

To develop the mathematical model of ASRR with the proper emission reflected from the spatially-distributed target, we consider the equivalent circuit presented in Fig. 1. Its resonant system (RS) is shown by a parallel tuned circuit, which contains the capacitor, the inductance and the conductance of own losses. At that, the capacitor represents a set of capacitances of the cavity itself, the permanent part of equivalent capacitances of AE and the varicap.

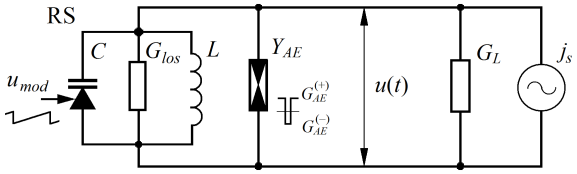

Fig. 1. The equivalent circuit of the autodyne transceiver module with simultaneous PAM and FM.

The load conductivity G_L and the signal current source $j_s \equiv j_s(t,\tau) = \sum_{k=1}^{K} j_k$ are connected in parallel with the tuned circuit. At that, G_L designates the input conductance of the antenna, and the current source – the impact to AD of the set of partial current sources $j_k \equiv j_k(t,\tau_k)$ caused by the reflected emission from the appropriate shining points (elementary reflectors) of the reflecting target (RT). Here $\tau_k = 2l_k/c$ is delay time of the reflected emission for the k^{th} shining point located on the l_k distance; c is the speed of radio wave propagation.

The AE of AD (for instance, the Gunn diode) in this circuit is also connected in parallel with RS on high frequency. In the general case, the Y_{AE} conductance of this element averaged over the oscillation period is the complex variable. It depends on the A amplitude, the current frequency ω: $Y_{AE}= G_{AE} + jB_{AE}$, where $G_{AE} \equiv G_{AE}(A,\omega)$, $B_{AE} \equiv B_{AE}(A,\omega)$ are reactive and reactive AE conductance, relatively. We shall assume then that during the pulse amplitude modulation of AD, the conductance G_{AE} varies. It has a positive value $G_{AE}^{(+)}$ when generation is absent, and becomes negative $G_{AE}^{(-)}$ when the excitation conditions in AD and formation of the probing radio pulse are created.

The main task of the considered model analysis is determination of time-laws of oscillation amplitude and frequency after AD activation during the time of radio pulse formation. To solve the task stated, we assume that the stationary oscillation mode settle down occurs during negligible small time compared to the minimal delay time τ_k. Taking into consideration the high enough loaded Q-factor $Q_L = \omega_r C/G$, where $G = G_{los} + G_L$, $\omega_r = (LC)^{-1/2}$ is the RS resonance frequency, we assume that oscillations on AE are quasi-harmonic. Then, an expression for output oscillations emitted by an antenna toward the radar target, beginning from the time $t = 0$, can be written in the general case as: $u(t) = \mathrm{Re}[A(t)\sigma(t)\exp j\Psi(t)]$. Here $\Psi(t) = \omega_0 t + \varphi$ is the AD full oscillation phase; $A = A(t)$, $\varphi = \varphi(t)$ are slowly-changed variables of amplitude and phase in the current time moment t; $\sigma(t)$ is the Heaviside function.

Oscillations reflected from the target and received by an antenna are quasi-harmonic as well. Let us present them as the set of partial current oscillations obtained from K shining points:

$$j_s = \mathrm{Re}\sum_{k=1}^{K} J_k(t,\tau_k)\ \sigma(\tau_k)\exp j\Psi_k(t,\tau_k), \qquad (1)$$

where $J_k(t,\tau_k)$, $\Psi_k(t,\tau_k)$ are the partial amplitude and phase of AD reflected oscillations from the kth shining point; $\sigma(\tau_k) \equiv \sigma(t=\tau_k)$ is the function $\sigma(t)$ shifted on τ_k time.

Usually, the wave amplitude, which is reflected from RT (1) and arrived into AD cavity, is significantly less than the amplitude of AD natural oscillations. Therefore, the further analysis of the autodyne response we perform in assumption of the small signal. For this case, according to known approach [9, 10], we obtain the system of differential equations with retarded argument for small amplitude relative variations $a = (A - A_0)/A_0$ and frequency variations $\chi = (\omega - \omega_0)/\omega_0$ of AD oscillations:

$$(Q_L/\omega_r)(da/dt) + \alpha\, a + \varepsilon\, \chi = \\ = \eta \sum_{k=1}^{K} \Gamma_k\, \sigma(\tau_k)\cos\delta_k, \qquad (2)$$

$$(Q_L/\omega_r)(d\varphi/dt) + \beta\, a + Q_L\, \chi = \\ = -\eta \sum_{k=1}^{K} \Gamma_k\, \sigma(\tau_k)\sin\delta_k, \qquad (3)$$

where α, ε, β are parameters defining the AD reduced increment slope, non-isodromity and non-isochronity, relatively [10]; $\Gamma_k \equiv \Gamma_k(t,\tau_k) = \Gamma_{0k}A_k(t,\tau_k)/A(t)$, $\delta_k \equiv \delta_k(t,\tau_k) = \Psi(t)\Psi_k(t,\tau_k)$ is a modulus and a phase of the instantaneous partial reflection factor on voltage from the kth shining point, which are reduced to AD terminals; $A_k(t,\tau_k)$, $\Psi_k(t,\tau_k)$ are amplitude and phase of AD oscillations in the time moment $(t-\tau_k)$; Γ_{0k} is the reflection factor characterizing the emission damping in amplitude at emission propagation to the kth shining point and back; $\eta = Q_L/Q_{ex}$, Q_{ex} is efficiency and external RS Q-factor.

At FM of autonomous oscillator by variation of bias voltage on the varicap, when $\Gamma_{0k} = 0$, both frequency $\omega_{FM}(t)$ and the spurious amplitude modulation (SAM) $A_{AM}(t)$ of emission [11]:

$$\omega_{FM}(t) = \omega_0 + \Delta\omega_{FM}(t) = \omega_0[1 + m_{FM} f_{mod}(t)], \quad (4)$$

$$A_{AM}(t) = A_0[1 + a_{AM}(t)] = A_0[1 + m_{AM} f_{mod}(t)] \quad (5)$$

where $m_{FM} = \Delta\omega_{FM}/\omega_0$ and $m_{AM} = \Delta A_{AM}/A_0$ are coefficients of FM and amplitude (AM) modulation,

relatively; $\Delta\omega_{FM}$, ΔA_{AM} are maximal deviations of amplitude and frequency from their stationary values A_0 and ω_0 due to modulation; $f_{mod}(t)$ is the normalized function , which frequency is Ω_{mod}.

Determination of the general solution of the equation system (2), (3) with account (4) and ((5) at arbitrary values of PAM and FM, and also values of Γ_k and δ_k at present seems to us as impossible. To continue this system examination, we assume that the least period of the autodyne response T_k is essentially more than the most delay time of the reflected emission τ_k, and also the transient period of the autodyne response $\tau_a = Q_L/\alpha\,\omega_0(1-\gamma\,\rho)$ [12]: $T_k >> \tau_k,\ \tau_a$. In addition, we suppose that the radio pulse repetition period T_{pul} is significantly more than the period of modulation function $T_{mod} = 2\pi/\Omega_{mod}$: $T_{pul} << T_{mod}$.

The first assumption permits to write: $\Gamma_k = \Gamma_{0k}$ [10]. Such an approximation in the ASRR mathematical model assumes taking into account of the phase delay only of the reflected emission. Other assumptions allow obtaining of the quasi-static [12] solution of the first approximation of (2) and (3) with account of (4) and (5). For this, supposing in (2) and (3) $da/dt = d\varphi/dt = 0$, we solve the obtained system of algebraic equations according to the Cramer method. Ass a result, we have expressions for the autodyne response on variation of the relative amplitude $a(t)$ and absolute values of frequency $\omega(t)$ in the form:

$$a(t) = m_{AM} f_{mod}(t) + K_a \sum_{k=1}^{K} \Gamma_k \sigma(\tau_k) \cos(\delta_k - \psi) \quad (6)$$

$$\omega(t) = \omega_0 \Bigg\{ 1 + m_{FM} f_{mod}(t) - \\ - L_a \sum_{k=1}^{K} \Gamma_k \sigma(\tau_k) \sin(\delta_k + \theta) \Bigg\}, \quad (7)$$

where $K = \eta(1+\rho^2)^{1/2}/\alpha(1-\gamma\rho)$, $L_a = \eta(1+\gamma^2)^{1/2}/Q_L(1-\gamma\rho)$ are coefficients of the autodyne amplification and the autodyne frequency deviation, relatively; $\psi = \arctan(\rho)$, $\theta = \arctan(\gamma)$ are angles of the phase offset of the autodyne response; $\rho = \varepsilon/Q_L$, $\gamma = \beta/\alpha$ are coefficients of non-isodromity and non-isochronity, relatively [10].

Then, let us consider the last terms in (6) and (7) defining useful components formation of the autodyne response. For these components, we have the normalized expressions for amplitude $a_n(t) = a(t)/\Gamma_\Sigma K_a$ (ACA) and frequency $\chi_n(t) = \chi(t)/\Gamma_\Sigma L_a$ (FCA) characteristics of the autodyne with PAM and FM in the form:

$$a_n(t) = \sum_{k=1}^{K} R_k \sigma(\tau_k) \cos(\delta_k - \psi) \quad (8)$$

$$\chi_n(t) = -\sum_{k=1}^{K} R_k \sigma(\tau_k) \sin(\delta_k + \theta) \quad (9)$$

where $R_k = \Gamma_k/\Gamma_\Sigma$ is the normalized modulus of the partial reflection factor fro kth shining point; $\Gamma_\Sigma = \sum_{k=1}^{K} \Gamma_k$ is the modulus sum of the partial reflection factors for K shining points of the target. ACA $a_n(t)$ and FCA $\chi_n(t)$ are the main ASRR characteristics defining a form and spectral composition of signals formed in AD [12]. We would like to note also that, starting from the normalization condition, the sum of R_k values over all k should be equal to 1.

According to the steps method [13], expressions (6), (7), (8), (9) permit to write the main relationships for calculation of absolute values of phase δ_k and frequency $\omega(t)$, as well as ACA $a_n(t)$ and FCA $\chi_n(t)$ of AD for the general case of emission impact from K shining points of the reflecting target.

Step 0. This step corresponds to the time interval $t \in (0, \tau_1)$ from the moment of oscillator activation to arrival of the first reflected emission. As in the case of the point reflector [13], in this case $\omega^{(0)}(t) = \omega_{FM}(t) = \omega_0 + \Delta\omega_{FM} f_{mod}(t)$ and $a^{(0)}(t) = m_{AM} f_{mod}(t)$, while $a_n^{(0)}(t) = \chi_n^{(0)}(t) = 0$. Thus, in this interval, we have, for each separate radio pulse, the steady-state mode depending only on the modulation function $f_{mod}(t)$. At that, the AD autodyne response is absent.

Hereinafter, indices in upper parenthesis at variables designate the step number.

Step 1. As a result of impact of the first ensemble of reflected emission from K shining points of the target, the autodyne variation of phase incursion happen of reflected emission from the separate reflectors $\delta_k^{(1)}$, the frequency $\omega^{(1)}(t)$, as well as AD ACA $a_n^{(1)}(t)$ and FCA $\chi_n^{(1)}(t)$ in the form of simple sums of separate components from (6), (7), (8), (9):

$$\delta_k^{(1)} = \omega^{(0)}(t)\,\tau_k = \omega_{FM}(t)\,\tau_k = \\ = [\omega_0 + \Delta\omega_{FM} f_{mod}(t)]\,\tau_k, \quad (10)$$

$$\omega^{(1)}(t) = \omega_{FM}(t) - \Delta\omega^m \sum_{k=1}^{K} R_k \sigma(\tau_k) \sin(\delta_k^{(1)} + \theta) = \\ = \omega_{FM}(t) - \Delta\omega^m \sum_{k=1}^{K} R_k \sigma(\tau_k) \sin[\omega_{FM}(t)\,\tau_k + \theta], \quad (11)$$

$$a_n^{(1)}(t) = \sum_{k=1}^{K} R_k \sigma(\tau_k) \cos(\delta_k^{(1)} - \psi) = \\ = \sum_{k=1}^{K} R_k \sigma(\tau_k) \cos[\omega_{FM}(t)\,\tau_k - \psi], \quad (12)$$

$$\chi_n^{(1)}(t) = \sum_{k=1}^{K} R_k \sigma(\tau_k) \sin(\delta_k^{(1)} + \theta) = \\ = \sum_{k=1}^{K} R_k \sigma(\tau_k) \sin[\omega_{FM}(t)\,\tau_k + \theta], \quad (13)$$

where $\Delta\omega^m = \sum_{k=1}^{K} \Delta\omega_k^m = \Gamma_\Sigma \omega_0 L_a$ are maximal autodyne frequency deviations at impact on AD of the set of all partial reflections from K shining points of the target; $\Delta\omega_k^m$ are the same but caused by reflection from the kth shining point.

Step 2. Oscillations changed at the first step, after delay on time of emission propagation to the reflector ensemble and back, affect on the oscillator, which oscillation parameters take new values of phase $\delta_k^{(2)}$, frequency $\omega^{(2)}(t)$, ACA $a_n^{(2)}(t)$ and FCA $\chi_n^{(2)}(t)$:

$$\delta_k^{(2)} = \omega^{(1)}(t)\,\tau_k = \\ = \omega_{FM}(t)\,\tau_k - \sum_{k=1}^{K} C_k^{FB} \sigma(\tau_k) \sin[\omega^{(0)}(t)\,\tau_k + \theta], \quad (14)$$

$$\omega^{(2)}(t) = \omega_{FM}(t) - \Delta\omega^m \sum_{k=1}^{K} R_k \sigma(\tau_k) \sin(\delta_k^{(2)} + \theta) = \\ = \omega_{FM}(t) - \Delta\omega^m \sum_{k=1}^{K} R_k \sigma(\tau_k) \sin[\omega_{FM}(t)\,\tau_k + \theta - \\ - \sum_{k=1}^{K} C_k^{FB} \sigma(2\tau_k) \sin[\omega_{FM}(t)\,\tau_k + \theta]], \quad (15)$$

$$a_n^{(2)}(t) = \sum_{k=1}^{K} R_k \sigma(\tau_k) \cos(\delta_k^{(2)} - \psi) = \\ = \sum_{k=1}^{K} R_k \sigma(\tau_k) \cos[\omega_{FM}(t)\,\tau_k - \psi - \\ - \sum_{k=1}^{K} C_k^{FB} \sigma(2\tau_k) \sin[\omega_{FM}(t)\,\tau_k + \theta]], \quad (16)$$

$$\chi_n^{(2)}(t) = \sum_{k=1}^{K} R_k \sigma(\tau_k) \sin(\delta_k^{(2)} + \theta) = \\ = \sum_{k=1}^{K} R_k \sigma(\tau_k) \sin[\omega_{FM}(t)\,\tau_k + \theta - \\ - \sum_{k=1}^{K} C_k^{FB} \sigma(2\tau_k) \sin[\omega_{FM}(t)\,\tau_k + \theta]], \quad (17)$$

where $C_k^{FB} = \Delta\omega^m R_k \tau_k = \omega_0 L_a \Gamma_k \tau_k$ is the partial parameter of ASRR feedback [14] caused by the impact of reflected emission from the kth shining point of the target; $\sigma(2\tau_k) = \sigma(t = 2\tau_k)$ hereinafter the figure before τ_k designates the multiplier of the time shift of τ_k for the $\sigma(t)$ function.

Step n. From (10), (11), (12), (13), (14), (15), (16), (17) we see that he impact result of $(n-1)$ reflected emission on the oscillation process analyzed at nth step can be written as:

$$\delta_k^{(n)} = \omega^{(n-1)}(t)\,\tau_k, \quad (18)$$

$$\omega^{(n)}(t) = \omega_{FM}(t) - \\ - \Delta\omega^m \sum_{k=1}^{K} R_k \sigma(n\,\tau_k) \sin(\delta_k^{(n)} + \theta), \quad (19)$$

$$a_n^{(n)}(t) = \sum_{k=1}^{K} R_k \sigma(n\,\tau_k) \cos(\delta_k^{(n)} - \psi), \quad (20)$$

$$\chi_n^{(n)}(t) = \sum_{k=1}^{K} R_k \sigma(n\,\tau_k) \sin(\delta_k^{(n)} + \theta). \quad (21)$$

Obtained expressions (10), (11), (12), (13), (14), (15), (16), (17), (18), (19), (20), (21) having the complicated tree-like form we use further for numerical analysis of ASRR signal properties with PAM and FM. Here, we would like to note additionally that the limitation is imposed upon values of the feedback parameter C_k^{FB} that a sum of C_k^{FB} values for all k should not exceed 1. Otherwise, the autodyne response formation can happen by jumps.

2 Calculation of Autodyne Signals

The main signal properties we examine on an example of target representation in the form of two shining points. At that, we choose the ratio of output signal periods and the modulation function period as multiplies in order to exclude influence of phase break points. We perform the signal analysis on the example of utilization in ASRR with PAM and FM of non-symmetrical saw-tooth law of the modulation function $f_{mod}(t) = (2/\pi)\tan^{-1}[\tan(\pi t)]$.

Calculation results of ACA in the form of time diagrams $a_n^{(n)}(t)$ and spectral characteristics $S_a^{(n)}(F_n)$ of autodyne signals on amplitude variations are presented in Fig. 2(b) – (e). Calculations of ACA $a_n^{(n)}(t)$ were performed according to (12), (16), (18), and (21) for different serial numbers n of reflected emission impact using the MathCad packet.

Figure 2(a), for better observation of current processes of signal formation, shows the time diagram $f_{mod}(t)$ and the spectral characteristic $S_{mod}(F_n)$ of modulating function. Here $S_a^{(n)}(F_n)$ and $S_{mod}(F_n)$ are spectral characteristics drawn for modulus of

amplitude coefficients of functions $a_n^{(n)}(t)$ and $f_{mod}(t)$ expansion into the Fourier series over the period of modulation function, accordingly; $F_n = 2\pi F/\Omega_{mod}$ is the normalized frequency.

Calculation results of FCA in the form of time diagrams $\chi_n^{(n)}(t)$ and spectral characteristics $S_\chi^{(n)}(F_n)$ of the autodyne response on the frequency variation are presented in Figs. 3(a) – (d). Calculations of FCA $\chi_n^{(n)}(t)$ were carried out according (11), (17), (18), and (21). Here $S_\chi^{(n)}(F_n)$ are spectral characteristics constructed for modulus of amplitude expansion coefficients of functions $\chi_n^{(n)}(t)$ in the Fourier series during the modulating function period.

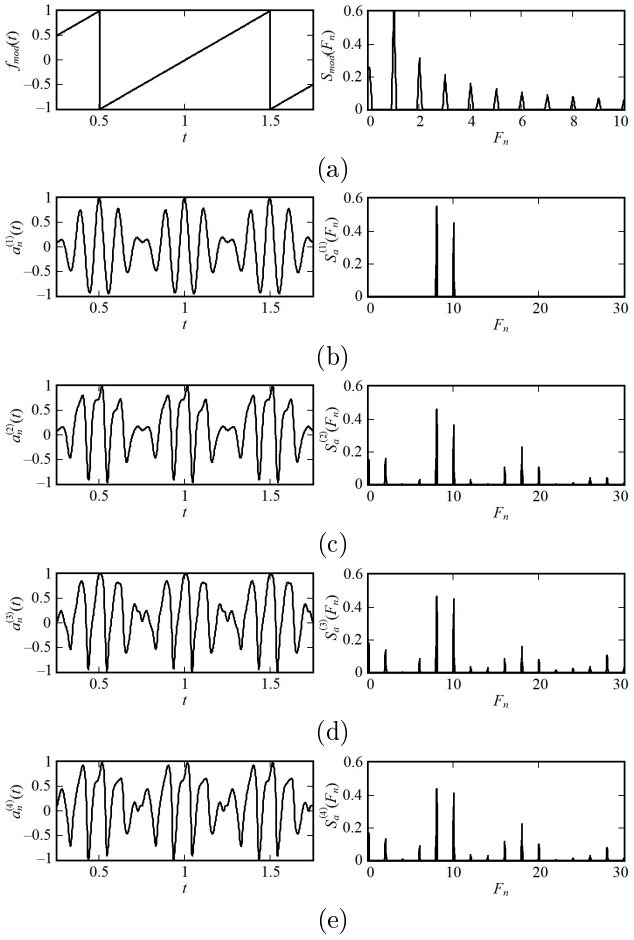

Fig. 2. Time diagrams of $f_{mod}(t)$, ACA $a_n^{(n)}(t)$ (left) and spectral characteristics $S_{mod}(F_n)$, $S_a^{(n)}(F_n)$ (right) of modulating function (a) and ASRR signals on amplitude variation for the case of PAM and FM calculated for different serial numbers n of reflected emission impact from two shining points: $n = 1$ (b), $n = 2$ (c), $n = 3$ (d) and $n = 4$(e).

Calculations of characteristics presented in Figs. 2 and 3 were performed for 8m-range oscillator, which frequency is $\omega_0 = 2\pi \times 37.5 \times 10^9$, the FM deviation is $\Delta\omega_{FM} = 2\pi \times 30 \times 10^6$, the offset angles of autodyne responses $\theta = 1$ and $\psi = -0.2$. It was assumed that two shining points in the form of elementary reflectors are located from ASRR at distances $l_1 = 20$m and $l_2 = 25$m. At that, ratios of proper amplitudes at ASRR input are: $R_1 = 0.55$, $R_2 = 0.45$, and partial AD feedback parameters are: $C_1^{FB} = 0.45$, $C_2^{FB} = 0.55$.

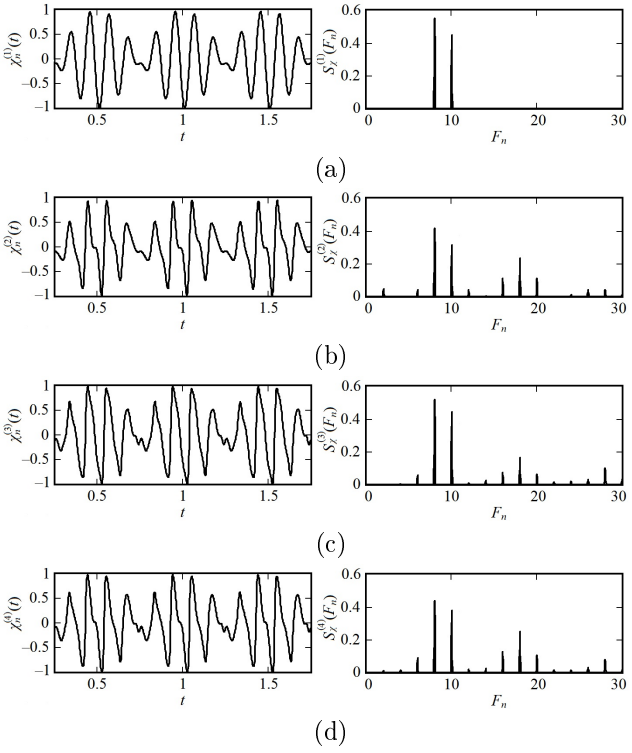

Fig. 3. FCA in the form of time diagrams $\chi_n^{(n)}(t)$ (left) and spectral characteristics $S_\chi^{(n)}(F_n)$ (right) of the autodyne response on frequency variations of ASRR with PAM and FM calculated for different serial numbers n of reflected emission impact from two shining points: $n = 1$(a), $n = 2$(b), $n = 3$(c), and $n = 4$(d).

From characteristics in Figs. 2(b) and 3(a) we see that at first step, the result of emission impact from separate shining points located at different distances represents the linear superposition of sine signals as it was in the homodyne systems. In this segment of the AD transient characteristic, the emitted and reflected oscillations of the radio pulse oscillator have no mutual dependence since here the oscillation frequency $\omega^{(0)}(t)$ varies only due to FM and the phase incursion $\delta_k^{(1)}$ linear related with delay time τ_k: $\delta_k^{(1)} = \omega^{(0)}(t)\,\tau_k$.

At second and following steps (see Fig. 2(c)–(e) and Fig. 3(b)–(d)) we clearly see manifestation of nonlinear interaction of partial signals obtained from different reflectors. As a result of such an interaction, the higher harmonics and sum, difference and combination components (besides the fundamental components) of the response are present in spectra $S_a^{(n)}(F_n)$ and $S_\chi^{(n)}(F_n)$ of resulting responses on amplitude $a_n^{(n)}(t)$ and frequency $\chi_n^{(n)}(t)$ variations, relatively. At that, differences of spectral characteristics $S_\chi^{(n)}(F_n)$ consists in absence of DC component and essentially less level

of harmonic components in the area of low (difference) frequencies than in the $S_a^{(n)}(F_n)$ spectrum.

Calculations of autodyne response characteristics at other initial conditions of ASRR with PAM and FM functioning, show the following. It is found out that reduction of the feedback parameter C_k^{FB} causes decrease of signal distortion obtained from separate shining points on the target and he degree of its nonlinear interaction. In the case, when the strong inequality $C_k^{FB} << 1$ is satisfied, we can neglect at all by the nonlinearity of ASRR with PAM and FM. This condition is the most effectively achieved by decrease of the frequency deviation $\Delta\omega_{\max}$, for instance, by application of frequency-tuned high-Q cavity in AD [15].

3 Experimental Results

Experimental investigations of signal features of ASRR with PAM and FM were executed with 8mm-range AD in the structure of the radar sensor developed for occupation monitoring of railroad crossing [5]. The module is made on the base of the Gunn diode AA727A and the varicap 3A637A-6. The output emission power was 50 mW, the central frequency was 37.5 GHz, the frequency deviation was 150 MHz, the FM frequency was 10 kHz, the PAM frequency was 500 kHz. We used the horn antenna with the pattern width 15×15 degrees. The functional diagram of the sensor is presented in Fig. 4.

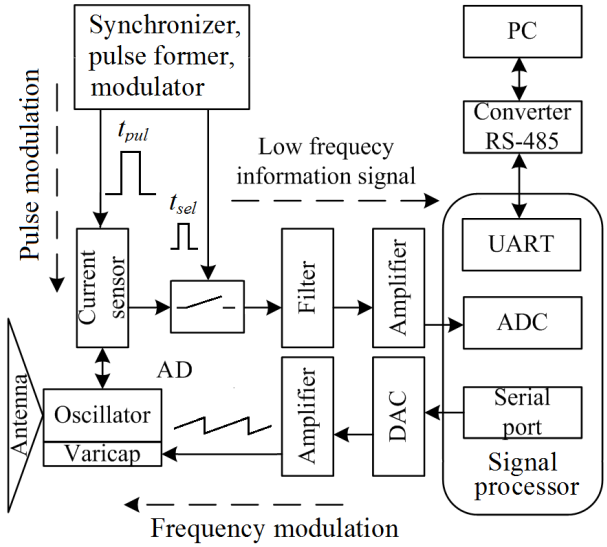

Fig. 4. Structural diagram of ASRR with PAM and FM.

Experimental investigations of ASRR signals PAM and FM were carried out in the following sequence. Two corner reflectors with the effective scattering cross-section about 10 m^2 were mounted on a tripod at distance $l_1 = 5$ m and $l_2 = 6$ m from the antenna aperture, which did not visually override each other in the antenna emission field. The first experiment was fulfilled at modulation pulse duration $t_{pul} = 50 \times 10^{-9}$ s, while the second – at $t_{pul} = 100 \times 10^{-9}$ s. At these duration values, the limited ranges $l_{\lim}$ of ASRR with PM action are accordingly: $l_{\lim .1} = 7.5$ m and $l_{\lim .2} = 15$ m.

Then, to determine the feedback parameter C_k^{FB} value, the AD was switched to the continuous wave mode, and at modulation absence, measurements of the autodyne frequency deviation were performed with the help the spectrum analyzer E4407B and the frequency converter. To execute these measurements, the mentioned instruments were connected through a directional coupler to the waveguide path between the AD output and the antenna. At these measurements fulfillment, the corner reflectors were in turn exposed to alternate-translational motion with respect to ASRR within the limits of several wavelengths. As a results, the autodyne frequency deviation for the first reflector was $\Delta\omega_1^m \approx 2\pi \times 2.4 \times 10^6$, while for the second – $\Delta\omega_2^m \approx 2\pi \times 1.5 \times 10^6$. At that, calculated values of AD feedback parameters are relatively: $C_1^{FB} \approx 0.5$ and $C_2^{FB} \approx 0.4$.

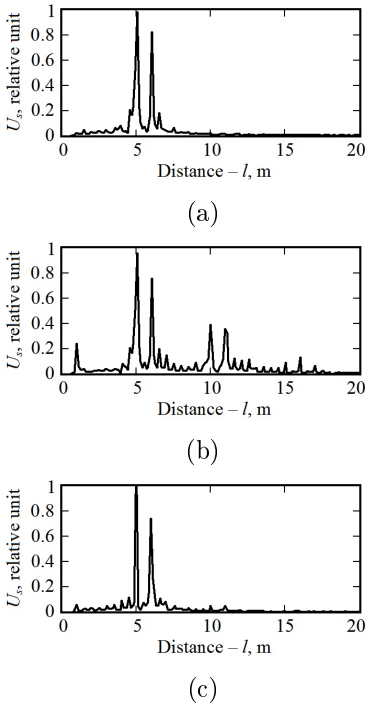

Fig. 5. Spectral characteristics of autodyne signals U_s of ASRR with PAM and FM obtained simultaneously from two reflectors in the antenna emission field for cases when modulation pulse duration $t_{pul} = 50 \times 10^{-9}$ s (a) and $t_{pul} = 100 \times 10^{-9}$ sec (b), and also at introduction of the additional signal attenuation in 10 dB (c) and $t_{pul} = 100 \times 10^{-9}$ sec.

Spectral characteristics of output signals U_s of the processing block of ASRR with PAM and FM obtained at execution of the first and the second experiments relatively are presented in Figs. 5(a) and (b). The case of autodyne signal formation obtained as a result of reception of the first set of partial reflections corresponds to the first experiment. The case of

signal formation obtained as a result of reception of first and right after the second set of partial reflections corresponds to the second experiment. In Fig. 5(c), the additional spectral characteristic is shown, which corresponds to the second case, but after introduction of additional attenuation of 10 dB into the waveguide path between AD and the antenna. As a result, AD feedback parameters had got the following values: $C_1^{FB} \approx 0.05$ and $C_2^{FB} \approx 0.04$, i.e., C_1^{FB}, $C_2^{FB} << 1$.

In the first case (see Fig. 5(a)), the main signal harmonics received from the corner reflectors are predominated on the spectral diagram. Nonlinear interaction between them is not practically observed. In the second case (see Fig. 5(b)), higher harmonic components and components of their nonlinear interaction take place. In the case of decrease of AD feedback parameters so that they become significantly less than 1, signal formation in the activity zone of two (and more) partial reflections from the target happens independently (linearly) as in SRR of homodyne type (see Fig. 5(c)).

From comparison of obtained characteristics in Figures 5(a) and (b) and characteristics presented relatively in Fig. 2(b) and (c), we see their qualitative agreement. From this, it follows that the experimental data obtained confirms an adequacy of above-developed mathematical model for analysis and calculation of signal and spectral characteristics of ASRR with PAM and FM.

4 Conclusion

Theoretical and experimental investigations performed in this paper show that at impact on ASRR with PAM and FM of the first ensemble of reflected emission from a set of shining points, which belong to the distributed radar target, the autodyne response spectrum represents the linear superposition of monochromic components obtained from separate points, as it is in system of homodyne type. The further impacts to AD of partial reflection ensembles cause the combination interaction of all spectral components between them. This is caused by autodyne frequency variations, which lead to nonlinearity of phase incursion of the reflected wave.

The manifestation degree of this nonlinearity is defined by value of total AD feedback parameter, which depends on both the reflected emission level and time of its propagation to reflectors and back. Besides, it follows from research performed that for reduction of autodyne signal nonlinear distortions and for widening of the dynamic range of radio pulse ASRR with FM, it is necessary to apply measures for frequency stabilization in oscillating modules, especially in mm-range. Solution of this problem is possible using the module, in which the frequency stabilization is achieved, for instance, with the help of high-Q cavity controlled in frequency [15].

Results obtained in this paper are evolved and added of results of earlier performed our researches in the part of FM and PAM account, on the case of AD interaction with reflected emission from the spatially-distributed target, which was not considered in [1].

Peculiarities of autodyne signals of radio pulse AD studied in the present paper for the first time were experimentally observed at testing of ASRR with PAM and FM, which was developed for monitoring of railroad crossing occupation [5]. The correct account of these features at a choice of modulation parameters and signal processing of ASRR developed by us, provide essential improvement of a series of its parameters. Manufactured ASRR samples show the high reliability of functioning under conditions of high traffic intensity through non-guarding railroad crossing, when the serious growth of passive interference is observed.

References

[1] Votoropin S.D., Noskov V.Ya., Smolskiy S.M. An analysis of the autodyne effect of a radio-pulse oscillator with frequency modulation. *Russian Physics Journal*, 2008, Vol. 51, No. 7, pp. 750–759. DOI: 10.1007/s11182-008-9105-3.

[2] Ivanov V.E., Noskov V.Ya. and Smolskiy S.M. (2009) Double-channel radio-pulse short-range radar on Gunn diode. *Microwave & Telecommunication Technology, CriMiCo 2009. 19th International Crimean Conference*, Sevastopol, pp. 817–820.

[3] Armstrong B.M., Brown R., Rix F., Stewart J.A.C. (1980) Use of Microstrip Impedance-Measurement Technique in the Design of a BARITT Diplex Doppler Sensor. *IEEE Transactions on Microwave Theory and Techniques*, Vol. MTT-28, No. 12, pp. 1437–1442. DOI: 10.1109/TMTT.1980.1130263.

[4] Varavin A.V., Vasiliev A.S., Ermak G.P. and Popov I.V. (2010) Autodyne Gunn-diode transceiver with internal signal detection for short-range linear FM radar sensor. *Telecommunication and Radio Engineering*, Vol. 69, No. 5, pp. 451–458. DOI: 10.1615/TelecomRadEng.v69.i5.80.

[5] Ermak G.P., Popov I.V., Vasiliev A.S., Varavin A.V., Noskov V.Ya. and Ignatkov K.A. (2012) Radar sensors for hump yard and rail crossing applications. *Telecommunication and Radio Engineering*, Vol. 71, No. 6, pp. 567–580. DOI: 10.1615/TelecomRadEng.v71.i6.80.

[6] Votoropin S.D., Donskov S.V., Noskov V.Ya. and Smolskiy S.M. (2007) Analysis of the autodyne signal from the distributed reflecting object. *Microwave & Telecommunication Technology, CriMiCo 2007. 17th International Crimean Conference*, Sevastopol, pp. 744–747. DOI: 10.1109/CRMICO.2007.4368928.

[7] Jefford P.A. and Howes M.S. (1985) Modulation schemes in low-cost microwave field sensor. *IEEE Transaction of Microwave Theory and Technique*, Vol. MTT-31, No. 8, pp. 613–624. DOI: 10.1109/TMTT.1983.1131559.

[8] Somekh M.G., Richmond W., Moroz J. and Lazarus M.T. (1980) Development of pulsed self-oscilating mixer. *Electronics Letters*, Vol. 16, No. 15, pp. 597–599. DOI: 10.1049/el:19800414.

[9] Takayama Y. (1973) Doppler signal detection with negative-resistance diode oscillators. *IEEE Transaction of Microwave Theory and Technique*, Vol. MTT-21, No. 2, pp. 89–94. DOI: 10.1109/TMTT.1973.1127929.

[10] Noskov V.Ya. and Ignatkov K.A. (2013) Autodyne signals in case of random delay time of the reflected radiation. *Telecommunication and Radio Engineering*, Vol. 72, No. 16, pp. 1521–1536. DOI: 10.1615/TelecomRadEng.v72.i16.70.

[11] Noskov V.Ya., Ignatkov K.A., Chupahin A.P., Vasiliev A.S., Ermak G.P. and Smolskiy S.M. (2016) Peculiarities of signal formation of the autodyne short-range radar with linear frequency modulation. *Visnyk NTUU KPI Seriia – Radiotekhnika Radioaparatobuduvannia*, No. 67, pp. 50–57.

[12] Noskov V.Ya. and Ignatkov K.A. (2014) About applicability of quasi-static method of autodyne systems analysis. *Radioelectronics and Communications Systems*, Vol. 57, No. 3, pp. 139–148. DOI: 10.3103/S0735272714030054.

[13] Noskov V.Ya. and Ignatkov K.A. (2013) Dynamics of autodyne response formation in microwave generators. *Radioelectronics and Communications Systems*, Vol. 56, No. 5, pp. 227–242. DOI: 10.3103/S0735272713050026.

[14] Usanov D.A. and Postelga A.E. (2011) Reconstruction of Complicated Movement of Part of the Human Body Using Radio Wave Autodyne Signal. *Biomedical Engineering*, Vol. 45, No. 1, pp. 6–8. DOI: 10.1007/s10527-011-9198-9.

[15] Kasatkin L.V. and Chaika V.E. (2006) *Semiconductor devices in the millimeter wave range*. Sevastopol, Veber, 319 p. (in Russian).

Особливості сигналів від розподілених відбиваючих об'єктів автодинного радіолокатора ближньої дії з одночасною імпульсною і лінійною частотною модуляцією

Носков В. Я., Ігнатков К. А., Чупахін А. П., Васильєв А. С., Фатєєв О. В., Смольський С. М.

Розроблено математичну модель для опису сигналів автодинного радіолокатора малого радіусу дії (АРМРД) з одночасною імпульсною модуляцією амплітуди (ІМА) і лінійною частотною модуляцією (ЧМ). Розглядаються особливості формування сигналів, отриманих від розподіленого об'єкта у вигляді ансамблю довільного числа точкових відбивачів. Виконано розрахунки сигналів запропонованим методом кроків для випадку двох точкових відбивачів на об'єкті локації, розташованих на різних відстанях від АРМРД. Встановлено відмінні властивості сигналів, які формуються у разі прийому першого і наступних випромінювань, що були відбиті від об'єкта локації. Результати експериментальних досліджень АРМРД з одночасною ІМА і лінійною ЧМ отримані під час використання генераторного модуля, що був виконаний на діоді Ганна 8-мм діапазону.

Ключові слова: автодин; автодинний ефект; автодинний сигнал; радіоімпульсний автодин; автодин з частотною модуляцією; параметр зворотного зв'язку; система ближньої радіолокації

Особенности сигналов от распределённых отражающих объектов автодинного радиолокатора ближнего действия с одновременной импульсной и линейной частотной модуляцией

Носков В. Я., Игнатков К. А., Чупахин А. П., Васильев А. С., Фатеев А. В., Смольский С. М.

Разработана математическая модель для описания сигналов автодинного радиолокатора малого радиуса действия (АРМРД) с одновременной импульсной модуляцией амплитуды (ИМА) и линейной частотной модуляцией (ЧМ). Рассматриваются особенности формирования сигналов, полученных от распределенного объекта в виде ансамбля произвольного числа точечных отражателей. Выполнены расчеты сигналов предложенным методом шагов для случая двух точечных отражателей на объекте локации, расположенных на различных расстояниях от АРМРД. Установлены отличительные свойства сигналов, формируемых при приёме первого и последующих излучений, отражённых от объекта локации. Результаты экспериментальных исследований АРМРД с одновременной ИМА и линейной ЧМ получены при использовании генераторного модуля, выполненного на диоде Ганна 8-миллиметрового диапазона.

Ключевые слова: автодин; автодинный эффект; автодинный сигнал; радиоимпульсный автодин; автодин с частотной модуляцией; параметр обратной связи; система ближней радиолокации